Split S-Shape Left Handed Metamaterial for Satellite Communication

Md. Mehedi Hasan[1,a], Mohammad Rashed Iqbal Faruque[1,b], Mohammad Tariqul Islam[2,c]

[1]Space Science Centre (ANGKASA), Universiti Kebangsaan Malaysia, Bangi 43600, Malaysia;

[2]Department of Electrical, Electronic and Systems Engineering, Faculty of Engineering and Built Environment, Universiti Kebangsaan Malaysia, Bangi 43600, Malaysia;

mehedi20.kuet@gmail.com[a], rashed@ukm.edu.my[b], tariqul@ukm.edu.my[c]

Abstract: In recent years, researchers have focused on satellite communications using metamaterials that are appropriate for X-band application. This paper presents a split S-shaped composed metamaterial that exhibits left-handed characteristics at the resonance frequency. The proposed metamaterial structure offers a bandwidth of almost 3.70 GHz at operating frequencies of 8.0 to 14.0 GHz. The fabricated structure also shows results similar to the simulation results. The metal strips of the outer ring resonator are split, and the inner ring resonator is designed so that it forms a split S-shaped structure that is printed on an epoxy resin fiber substrate. CST Microwave Studio electromagnetic simulator is used for design and simulation, and the NRW method is used to characterize the designed metamaterial. The total dimensions of the unit cell structure are $0.4\lambda \times 0.4\lambda \times 0.06\lambda$, and an Agilent N5227A vector network analyzer is used to validate the measurements.

Keywords: Capacitive effect, Inductive effect, Left handed, Metamaterial.

1. Introduction

Metamaterials are composed of periodic metal or dielectric structures that are resonantly coupled to the electric and magnetic components of the incident electromagnetic field and show unusual properties that are not available in nature. This class of micro structured artificial materials has attracted great interest during the past 15 years for their otherwise inaccessible electromagnetic properties, such as negative refractive index, negative permittivity, negative permeability, etc. Material with negative permittivity, permeability and smaller wave length, than the target wave length for specific application are the extraordinary phenomena's of the metamaterials. Metamaterial with negative permittivity (ε) and permeability (μ) was first shown by Veselago et al. in 1968 [1]. After a long time, simultaneously negative permittivity (ε) and permeability (μ) was successfully invented by Smith et al. in 2000 [2]. Material either negative permittivity or permeability ($\varepsilon<0$ or $\mu<0$) is called single negative metamaterial. When the value of permittivity and permeability are near zero ($\varepsilon\approx0$ and $\mu\approx0$) over a specific frequency range then the material is specified as near zero refractive index metamaterial. Moreover, material with simultaneously negative permeability and permittivity ($\varepsilon<0$ and $\mu<0$) can be characterised as left handed metamaterial. From the past age, different shape and structural metamaterial have been utilized for several applications, like [3-5], antenna design, electromagnetic absorber, invisible cloaking operation, sensing applications, etc. Moreover, the design of antennas for advanced technologies requires antennas that operate easily, large bandwidth, high transmission capacity and maintaining a compact size. Although patch antennas suffer from narrow bandwidths, parasitic patches have been used to increase bandwidths of patch antennas.

However, due to large bandwidth, transmission capacity, gain, directivity, short range features, many different alphabetical shapes now metamaterials are using for satellite applications. Novak et al. designed an ultra-wideband array of antenna for UHF, L-, S-, and Lower-C bands (from 0.6 to 3.6 GHz), as well as achieves a minimum 6:1 bandwidth for VSWR less than 1.8, 2.4, and 3.1 for 0^0, 45^0, and 60^0 scans, respectively in 2015 [6]. An aperture antenna for simultaneous operation in L- and Ka-band was demonstrated by Smith et al. in 2014. This antenna consisted of a reflect-array antenna with a frequency selective surface ground-plane. The reflect-array provided a maximum directivity of 36.4 and 38.5 dBi in 20.0 and 29.8 GHz, respectively, and an aperture illumination efficiency in the two frequency bands up to 57% and 48%, respectively [7]. A metamaterial inspired symmetrical slotted patch antenna for tri-band operation, where after inclusions of the metamaterial the bandwidth increment was 12.43% and size reduction was obtained up to 36.7% [8]. A SRR array-loaded microstrip patch antenna was presented for defence communication applications operating in L- and S-bands. The proposed antenna was flexible in tuning along with simultaneous achievement of required gain and cross-polarization levels for the satellite applications [9]. Perez et al. proposed a performance improvement of a planar antenna array system by metamaterial approach in 2015. At last, the gain of the improved antenna resulted in 6.8 dBi, resulting in +1.6 dB without external components. However, by simply using this approach a saving of space of 41% is achieved [10]. Later, an "S-shape" 15×15 mm^2 dimension chiral metamaterial for X- and Ku-band but the effective medium ratio was less than 4 was introduced by Zhimou et al. in 2015 [11]. A "Ring-shape" meta-atom for wearable microwave meta-skin and cloaking effects from 8.0 to 10 GHz was suggested by Yang et al. in 2016 [12]. However, a modified double negative "Z-shaped" metamaterial was developed for wide band operation but the bandwidth was 2.17 GHz (from 7.87 to 10.04 GHz). This metamaterial structure was compact in size and applicable for C and X-band applications was proposed by Hasan et al. in 2016 [13].

In this paper, the designed metamaterial structure is consisting of a split S-shape ring resonator with an outer square shape ring resonator of copper. The proposed unit-cell exhibits resonances at X-band with negative refractive index from 8.0 to 11.70 GHz and 11.78 to 14.0 GHz, bandwidth covers respectively 3.70 GHz and 2.22 GHz. These X-band is applicable for the satellite communications. The proposed metamaterial shows larger bandwidth than the reference prototypes [8-13] and exhibits left handed characteristics at the resonance frequency. Besides, here a parametric study on substrate material has been analysed to demonstrate the effects on resonance frequency by the inductance and capacitance. By increasing, the length or width of the substrate material inductive effect is also raised and resonance frequency is decreased. Consequently, by decreasing the length or width of the substrate material raise capacitance and capacitive effect shifted the resonant frequency downwards. So, the inductive and capacitive effect are created by varying the length or width of the substrate materials elaborately discussed by tables and figures in the results section. Besides, a metamaterial is a material which gains its properties from its structure rather than directly from its composition. As a result, by inclusion of these proposed metamaterial, the antenna performance can be raised for the satellite applications. The parameters of the proposed metamaterial unit-cell are,

Table 1. Design parameters of split S-shape metamaterial single unit cell.

Parameters	a	b	L	w	d	g	G	h
Dimensions (mm)	10	10	8.0	8.0	0.5	0.5	0.3	0.035

Epoxy resin fibre is used as substrate material, which dielectric constant, loss tangent and thickness are respectively 4.5, 0.002 and 1.6 mm. However, the dimension of are unit cell is 10×10 mm^2 and the unit cell structure is specified in figure 1(a-b).

2. Methodology

Finite integration technique (FIT) based CST Microwave Studio is used to observe the reflection (S_{11}) and transmission (S_{21}) coefficients of the proposed metamaterial to calculate the effective medium parameters. In the simulation and measurement technique the unit-cell structure is placed between two waveguide ports and the direction of electromagnetic wave propagation is set to the z-axis. Perfect electric and perfect magnetic boundaries are also considered at the x- and y-axis. Frequency domain solver with tetrahedral mesh have been utilized for simulation purpose. However, the operating frequency ranges for the proposed meta-atom structure is from 8.0 to 14.0 GHz, whereas the impedance has been set to 50 ohms. The boundary condition in the simulation of the proposed metamaterial is given in Figure 2(b).

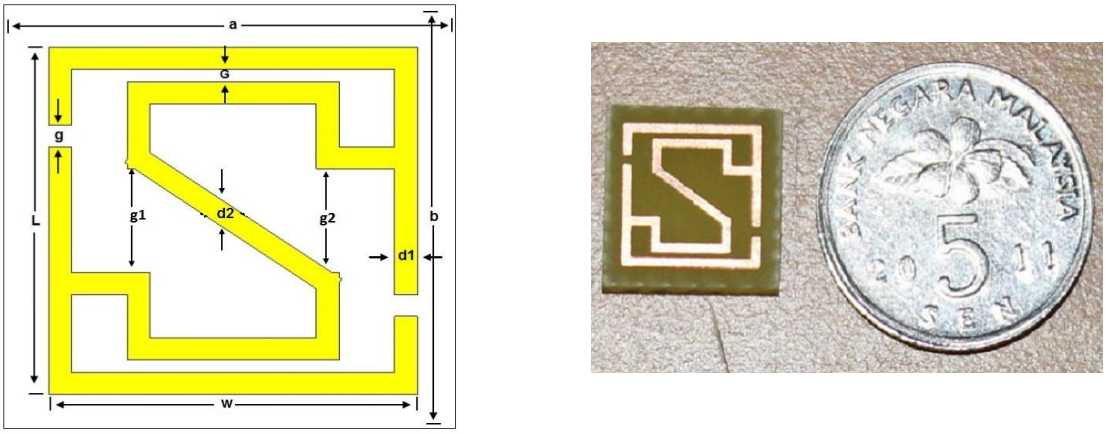

(a) (b)

Figure 1. Proposed unit-cell: (a) Schematic structure, (b) Fabricated structure.

For understanding the electromagnetic behaviours of the proposed unit cell, effective medium parameters are figure out from the reflection (S_{11}) coefficient and transmission (S_{21}) coefficient. So, the effective permittivity (ε_r), permeability (μ_r) and refractive index (n_r) are acquired by [13],

$$\varepsilon_r = \frac{c}{j\pi f d} \times \left\{ \frac{(1 - S_{21} - S_{11})}{(1 + S_{21} + S_{11})} \right\} \quad (1)$$

$$\mu_r = \frac{c}{j\pi f d} \times \left\{ \frac{(1 - S_{21} + S_{11})}{(1 + S_{21} - S_{11})} \right\} \quad (2)$$

$$n_r = \frac{c}{j\pi f d} \times \left\{ \frac{(S_{21}-1)^2 - S_{11}^2}{(S_{21}+1)^2 - S_{11}^2} \right\}^{1/2} \tag{3}$$

The resonance frequency of the proposed metamaterial is,

$$f = \frac{1}{2\pi\sqrt{L_T C_T}} \tag{4}$$

Here, L_T and C_T are the total inductance and capacitance. Inductances are formed by the metal strips and the capacitances are formed by the gaps in the designed structure. The total inductance (L_T) for the proposed metamaterial can be obtained by,

$$L_T = 0.01 \times \mu_0 \left\{ \frac{2(d+g+h)^2}{(2w+g+h)^2} + \frac{\sqrt{(2w+g+h)^2 + l^2}}{(d+g+h)} \right\} t \tag{5}$$

However, the total capacitance (C_T) can be calculated by,

$$C_T = \varepsilon_0 \left[\frac{(2w+g+h)}{2\pi(d+h)^2} ln \left\{ \frac{2(d+g+h)}{(a-l)} \right\} \right] t \tag{6}$$

where, the free-space permeability (μ_0) is $4\pi \times 10^{-7}$ H/m and the permittivity (ε_0) is 8.85×10^{-12} F/m.

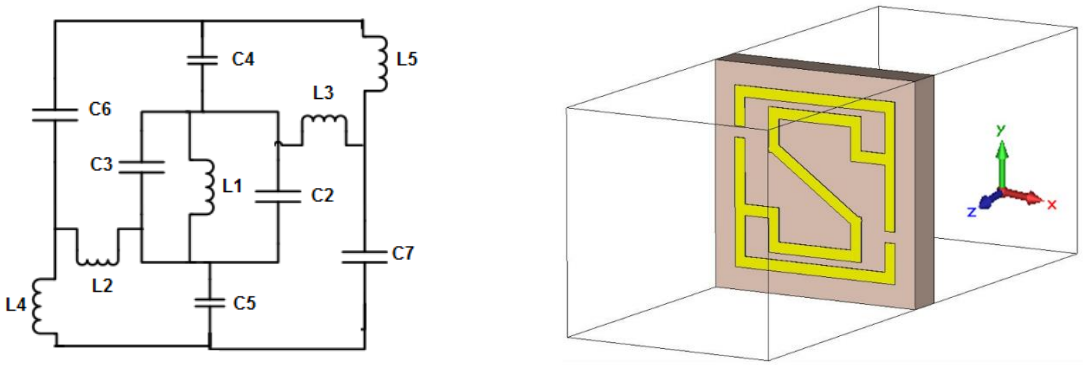

(a) (b)

Figure 2. (a) Equivalent circuit model of the split S-shape structure, (b) Boundary condition and simulated structure of the proposed metamaterial unit cell in the CST-Microwave Studio.

In the above figure 2(a), the series and shunt branch of the circuit are responsible for the inductance and capacitance. The splits are maintained capacitive effect denoted by C1, C2, C3, C4, C5, C6 and C7 in circuit. Similarly, metal strips are creating inductive effect symbolized by L1, L2, L3, L4 and L5. For adding more split in designed metamaterial structure produce a small phase delay and reduce the capacitive effect. Due to reduce capacitance the split S-shape unit cell shows resonance at higher frequency. The measurement is performed by placing the prototype between the waveguide ports. An Agilent N5227A vector network analyser is utilized to determine the S-parameters of the split S-

shape structure. However, Agilent N4694-60001 is also used to calibrate the N5227A-VNA for performing the measurement accurately.

3. Results & Discussions

The current distribution, electric field and magnetic field distribution of the unit cell at 11.92 GHz are shown in figure 3(a-c). The currents are flowing towards the forward and reverse direction in the same resonator metal strip of the unit cell because of the dissimilar geometry of the proposed structure. Due to flow opposite currents in the inner and outer surface cause stop band at resonance frequency range.

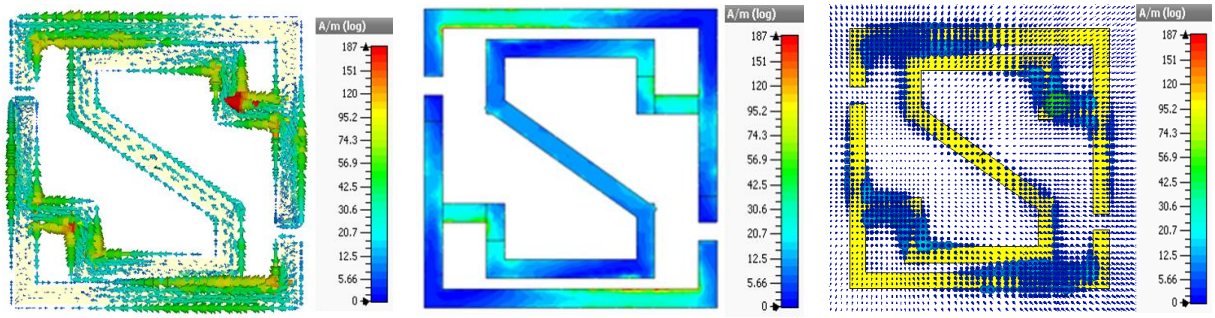

(a) (b) (c)

Figure 3. (a) Surface current distribution at 11.92 GHz, (b) Electric field distribution at 11.92 GHz, (c) Magnetic field distribution at 11.92 GHz.

Figure 4, shows resonance at 12 GHz is simulation result but resonance at 11.92 GHz (X-Band) in the same figure is the measured result. However, simulated and measured resonance are almost well compiled but measure result slightly shortened and shifted than the simulated results. This shift usually occurs due to the interference, fabrication tolerance.

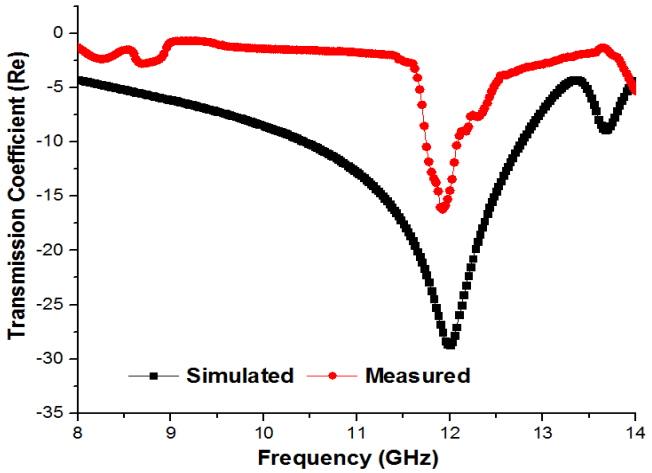

Figure 4. Transmittance (S_{21}) coefficient of the proposed split s-shape metamaterial.

Figure 5, indicates the real value of the effective medium parameters. In Figure 5(a), negative permeability (μ) from 10.70 to 14.0 GHz covers bandwidth 3.30 GHz. Normally, the frequency ranges at which the permeability of the unit cell is negative current can keep pace with the applied field at lower frequency but at higher frequency the current cannot cope with the applied field and start lagging. Moreover, from 8.0 to 14.0 GHz the values of permittivity

(ε) are negative but almost near zero. Here it reveals that there is a variation between the permeability and permittivity because of the polarization affect due to internal manner of the material. When the electromagnetic waves enter inside of the materials. If the unit cell permittivity and permeability appears negative simultaneously then the refractive index curve would be negative. However, the proposed unit cell structure exhibits simultaneously negative permittivity and permeability from 10.70 to 14.0 GHz. As expected, the proposed metamaterial shows real magnitude of negative refractive index (n) from 8.0 to 11.70 GHz and 11.78 to 14.0 GHz, respectively covers bandwidth 3.70 GHz and 2.22 GHz in figure 5(b). At resonance 11.92 GHz effective permittivity, permeability and refractive index are negative and the values are recorded in table 2. As a result, this split S-shape metamaterial structure can be characteristics as a left handed metamaterial.

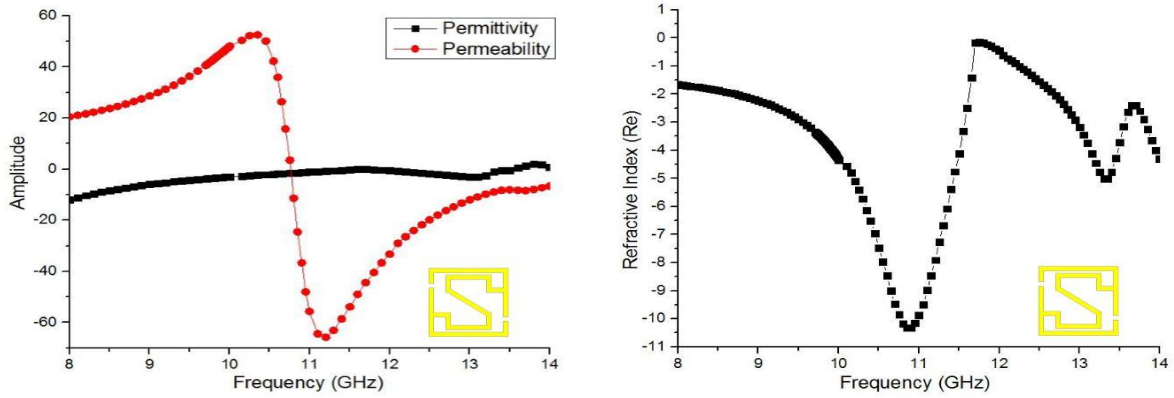

(a) (b)

Figure 5. Real magnitude of: (a) effective permittivity (ε) & permeability (μ) vs. frequency, (b) effective refractive index (n) vs. frequency of the proposed metamaterial.

3.1 Effect of Substrate Material

Three different size of unit cells (8×8 mm^2, 10×10 mm^2 and 12×12 mm^2) are designed to investigate the effect of the unit cell size on the resonance frequency. If the dimension of the substrate material is increased, then inductive effect is also increased and resonance frequency is declining. Similarly, by decreasing the dimension of the substrate material capacitive effect can be raised for the proposed structure and shifted the resonance towards the higher frequency. From Table 2, resonance frequencies are shifted to the lower frequency with the increase of the structure size. Similarly, for smaller size unit cell resonance becomes at higher frequencies. Moreover, for 8×8 mm^2, 10×10 mm^2 and 12×12 mm^2 dimension unit cell structures resonance frequencies are respectively 13.25 GHz, 12 GHz and 8.60 GHz shown in figure 6(a).

Table 2. Relationship between the unit-cell dimension and the resonance frequency.

Unit cell Dimension (mm^2)	Resonance Frequency (GHz)	Max. Value of Transmittance
8×8	13.25	-32.28
10×10	12.00	-28.71
12×12	8.60	-18.93

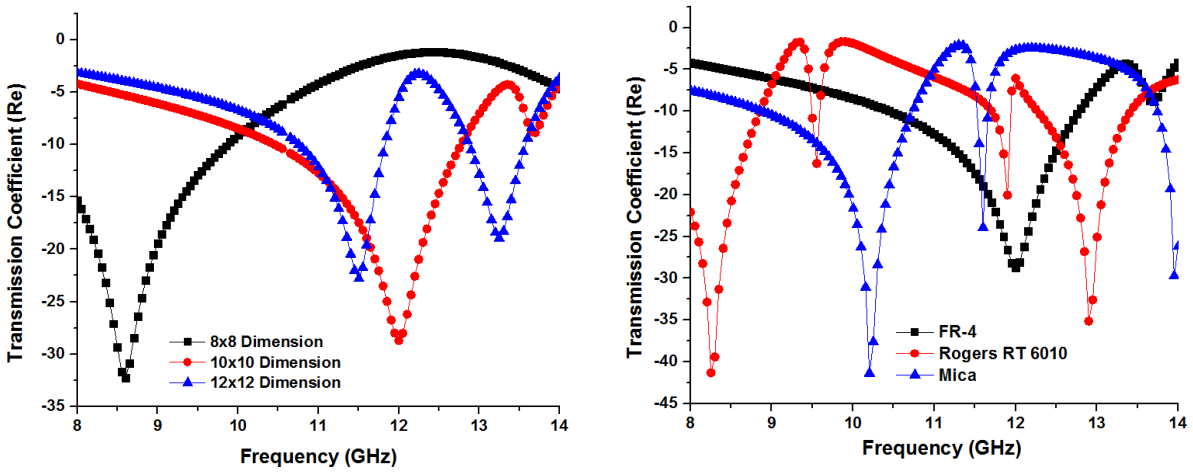

(a) (b)

Figure 6. Relation between the effects of substrate materials: (a) dimension vs. resonance frequency; (b) different substrate material vs. resonance frequency.

Figure 6(b) represents the effect on resonance frequency by different types of substrate materials. In addition, the dielectric constant and tangent loss of the FR-4, Rogers RT 6010, Mica are respectively 4.5, 10.6, 5.4 and 0.002, 0.0023, 0003. For the substrate material dielectric constant is a very important factor. If the dielectric constant is increased, then substrate material conductivity is decreased. The dielectric constant of a material depends on the material internal structure. When electromagnetic waves propagated through a material and its electric and magnetic fields oscillate as sinusoidal pattern and its velocity depends upon material electrical conductivity, which actually depends on material internal structure. Electrical signals are travel through the material varies by relative speed, according to the sort of interaction with its internal structure. However, the variation in the inner metallic pattern are caused the different results in the transmission characteristics. From table 3, resonance at 12 GHz for FR-4, at 10.20 GHz and 13.95 GHz for Mica as well as at 8.25 GHz, 11.90 GHz, 12.90 GHz for Rogers RT 6010.

Table 3. Relationship between the different substrate material and resonance frequency.

Substrate Material	Dielectric Constant	Resonance Frequency	Max. Value of Transmittance (S_{21})
Fr-4	4.5	12.00 GHz	-28.71
Mica	5.4	10.20 GHz 13.95 GHz	-41.37 -29.71
Rogers RT 6010	10.2	8.25 GHz 11.90 GHz 12.90GHz	-41.31 -20.05 -35.15

From table 4, the designed metamaterial bandwidth is 3.70 GHz, which is almost triple than the ref. [8]. However, the bandwidth is increased almost 12.16%, 61.89%, 28.38%, and 58.64% respectively in the ref. [9-13].

Table 4. Performance analysis of the proposed metamaterial with the previous researches.

References	Bandwidth (GHz)	Bandwidth Increase (%)
Zhou et al. [11]	9.71 to 12 GHz (bandwidth of 2.29 GHz)	61.89 %
Yang et al. [12]	9.30 to 10.35 GHz (bandwidth of 1.05 GHz)	28.38 %
Hasan et al. [13]	7.87 to 10.04 GHz (bandwidth of 2.17 GHz)	58.64 %
Proposed Metamaterial	8 to 11.70 GHz (bandwidth of 3.70 GHz)	100 %

4. Conclusion

In this paper, simulation and fabrication of a split S-shaped metamaterial structure printed on epoxy resin fiber is reported; the structure shows left-handed characteristics at 11.92 GHz. The designed metamaterial is miniaturized, well-matched, flexible, and easy to manufacture. Simulated and experimental results show excellent agreement, suggesting that the metamaterial performs very well in much of the X- band. The proposed structure exhibits resonance at 11.92 GHz and a bandwidth of almost 3.70 GHz (from 8.0 to 11.70 GHz). The effect of the substrate material on the resonance frequency is also investigated, and the inductive and capacitive effects are explained in detail. Finally, the designed X-band metamaterial can be applied in satellite communication and space communication.

References

[1] Veselago, V. G.; "The electrodynamics of substances with simultaneously negative values of ε and μ", *Sov. Phys.*, **1968**, Vol. 10, pp. 509-514.

[2] Smith, D. R.; Padilla, W. J.; Vier, D. C.; Nemat- Nasser, S. C.; Schultz, S.; "Composite medium with simultaneously negative permeability and permittivity", *Physical Review Letters*, **2000**, Vol. 84, pp. 4184-4187.

[3] Smyth, B.; Barth, S.; Iyer, A. K.; "Dual-band Microstrip Patch Antenna Using Integrated Uniplanar Metamaterial-Based EBGs", *IEEE Transactions on Antennas and Propagation*, **2016**, DOI: 10.1109/TAP.2016.2618854.

[4] Hasan, M. M.; Faruque, M. R. I.; Islam, M. T.; "Multiband Left Handed Biaxial Meta Atom at Microwave Frequency", Material research express, **2017**, Vol. 4, No. 3, doi: 10.1088/2053-1591/aa61cd.

[5] Ozbey, B.; Ertürk, V. B.; Kurc, O.; Altintas, A.; Demir, H. V.; "Multi-Point Single-Antenna Sensing Enabled by Wireless Nested Split-Ring Resonator Sensors", *IEEE Sensors Journal*, **2016**, Vol. 16, No. 21.

[6] Novak, M. H.; Volakis, J. L.; "Ultra wideband Antennas for Multiband Satellite Communications at UHF–Ku Frequencies", IEEE Transactions on Antennas and Propagation, **2015**, doi: 10.1109/TAP.2015.2390616.

[7] Smith, T.; Gothelf, U.; Kim, O. S.; Breinbjerg, O.; "An FSS-Backed 20/30 GHz Circularly Polarized Reflectarray for a Shared Aperture L- and Ka-Band Satellite Communication Antenna", IEEE Transactions on Antennas and Propagation, **2014**, Vol. 62, No. 2.

[8] Dwivedi, S.; Mishra, V.; Kosta, Y. P.; "Metamaterial Inspired Patch Antenna Minituration
Technique for Satellite", International Conference on Emerging Technology Trends in Electronics, Communication and Networking, **2012**.

[9] Upadhyaya, T. K.; Kosta, S. P.; Jyoti, R.; Palandoken, M.; "Novel stacked m-negative material-loaded antenna for satellite applications", International Journal of Microwave and Wireless Technologies, pp. 1-7, doi: 10.1017/S175907871400138X.

[10] Perez, G. E.; "Enhancement of Beam forming Antenna Array using a CSRR Metasurface for Satellite Applications", International Congress on Advanced Electromagnetic Materials in Microwaves and Optics – Metamaterials, **2015**.

[11] Zhou, Z.; Yang, H.; "Triple-band asymmetric transmission of linear polarization with deformed S-shape bilayer chiral metamaterial" *Appl. Phys. A,* **2015**.

[12] Yang, S.; Liu, P.; Yang, M.; Wang, Q.; Song, J.; Dong, L.; "From flexible and stretchable meta-atom to metamaterial: a wearable microwave meta-skin with tunable frequency selective and cloaking effects", *Sci. Rep.*, 6, **2016,** article number- 21921.

[13] Hasan, M. M.; Faruque, M. R. I.; Islam, S. S.; Islam, M. T.; "A New Compact Double-Negative Miniaturized Metamaterial for Wideband Operation", *Materials*, **2016**, 9(10), 830.